Available online at www.sciencedirect.com
SCIENCE DIRECT®
Polymer 45 (2004) 3465–3471
polymer
www.elsevier.com/locate/polymer

Micropatterning from drying micelle solution of diblock copolymers: strap-structure, quadrate farmland-structure and biomimetic structure

Yannie Chan[a], Xiaolin Lu[a], Er Qiang Chen[b], Yongli Mi[a,*]

[a]*Department of Chemical Engineering, Hong Kong University of Science and Technology, Clear Water Bay, Kowloon, Hong Kong, China*
[b]*Department of Polymer Science and Engineering, College of Chemistry, Peking University, Beijing, China*

Received 10 March 2003; received in revised form 17 September 2003; accepted 19 September 2003

Abstract

Micropatterns of strap and farmland structures of polystyrene-block-poly(acrylic acid) (PS-*b*-PAA) copolymer were obtained by drying the micelle solutions. The drying process of the solution was monitored by dynamic optical microscopy (OM) with a digital video camera. The surface structure of the micelle aggregations was studied by OM, scanning electron microscopy and Alpha-Step 200 profiler system. It is believed that solvent evaporation and micelle migration account for the observed micelle micropatterns. The potential application of the micropatterns is also addressed.

Keywords: Diblock copolymer micelles; Scanning electron microscopy; Micropatterning

1. Introduction

The self-assembly of amphiphilic block copolymers has been widely investigated for years. Various morphologies and phase structures with self-assembly, such as spherical, cylindrical, bicontinuous and lamellar, have been observed in different block polymers [1]. Microstructures of spheres, rods, lamellae and vesicles have also been observed in micelle solutions [2–5]. Microstructures of diblock copolymer are related to their special characteristics and the study of diblock copolymers is important to the research in micropatterning [6–9], nanotechnology, lithography [10–13], and bioengineering [14–19].

Different methods for the preparation of polymer micelles have been reported [3,20–22]. In 1995, Zhang and Eisenberg reported the observation of the needle-like patterning of the diblock copolymer PS_{310}-*b*-PAA_{52} [2]. However, the mechanism of the formation of such structure has not been studied. Recently, we found that the needle-like pattern, or more precisely, the strap structure, found by Zhang and Eisenberg [2], is only an unstable intermediate state when the micelle solution is dried. More regular farmland structures can be developed as shown in Fig. 1(A)–(D). It is observed that when micelle solution was dropped on the surface of a coverglass and was allowed to evaporate, micron-sized strap patterns and farmland patterns could be obtained. These structures appeared to be regularly developed during the solvent evaporation process. A method of microfabrication and micropatterning could be developed by considering the mechanism of this drying process. Fig. 1(A) shows the strap structure thus obtained. The two arrows in Fig. 1(B) indicate the starting formation of the farmland structure. Fig. 1(C) shows the nearly complete farmland structure. Fig. 1(D) demonstrates the farmland structure.

2. Experimental

The amphiphilic diblock copolymer used in this study was polystyrene-block-polyacrylic acid (PS-*b*-PAA), which was purchased from Polymer Source, Inc., Quebec, Canada. This polymer has the block molecular weights of M_n(PS) = 66,500 and M_n(PAA) = 4500. The polymer was dissolved in the common solvent THF at the concentrations

* Corresponding author. Tel.: +852-2358-7127; fax: +852-2358-0054.
E-mail address: keymix@ust.hk (Y. Mi).

0032-3861/$ - see front matter © 2004 Elsevier Ltd. All rights reserved.
doi:10.1016/j.polymer.2003.09.068

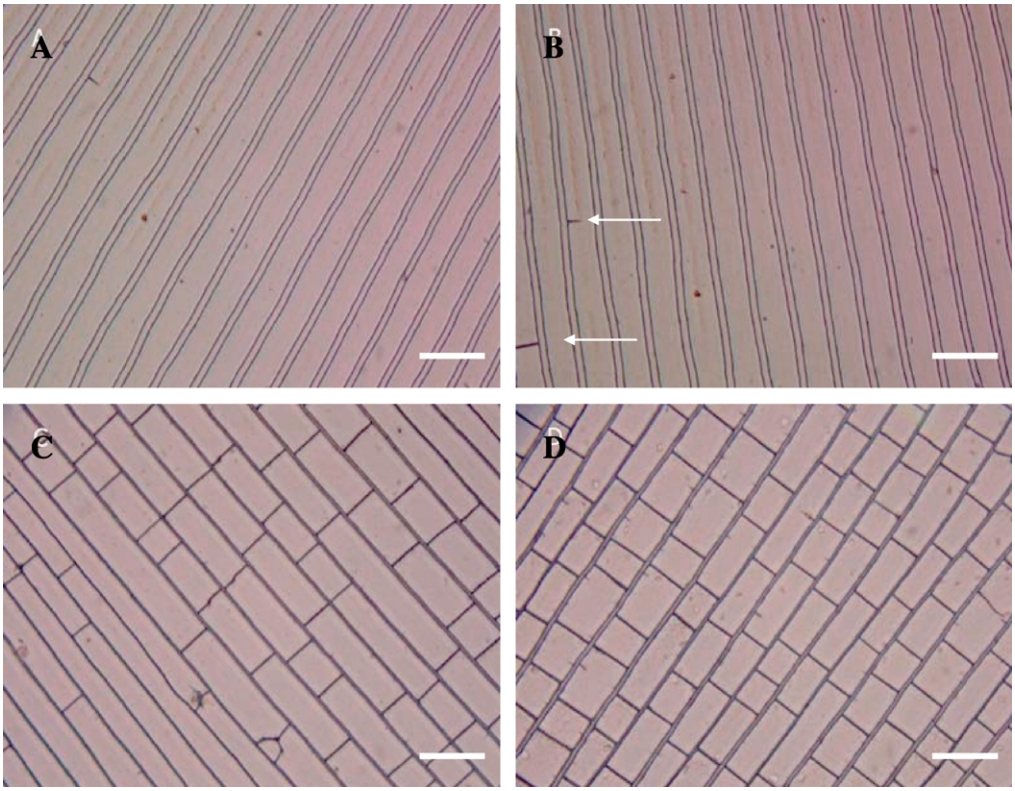

Fig. 1. Optical microscopic images of strap structure (A), the starting phase of farmland structure (B), the nearly complete farmland structure (C), and the final micropatterns of farmland structure (D). (The scale bar on the graphs is 50 μm.)

of 1, 5, and 10 mg/ml. Deionized water was used as the selective solvent for the PAA block and was added at a volume ratio of 1:10 (water:THF) with mild stirring. After overnight stirring, a stable micelle solution was obtained. The micelle solution was dropped on the surface of a coverglass and was observed under an optical microscope (Leica DMLM, Germany). The dried patterns on the coverglass were then coated with a gold layer for scanning electron microscopy (SEM) (Jeol 6300) examination.

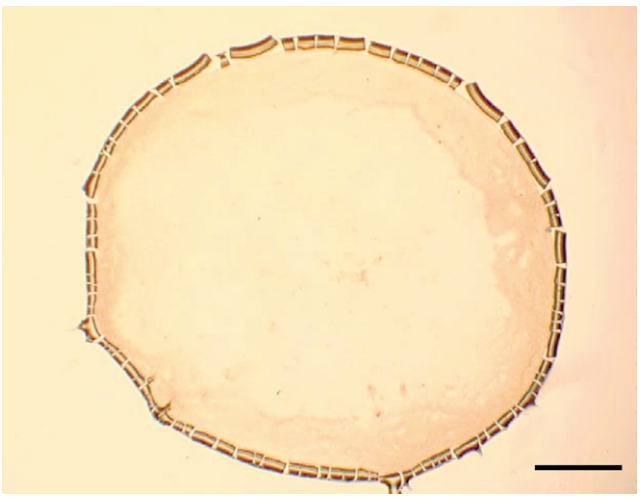

Fig. 2. The ring-form drying pattern of a droplet of PS-*b*-PAA micelle solution of 1 mg/ml. (The scale bar on the graph is 500 μm.)

3. Results and discussion

After a droplet of micelle solution of low concentration (1 mg/ml) was cast onto the coverglass and was left drying, a ring-shaped stain of dried micelle aggregate was observed under an optical microscope as shown in Fig. 2. The mechanism of such ring-shaped pattern formation, which has been discussed by Deegan et al. in a study of the formation of ring-formed coffee stain, was attributed to the capillary flow of the drying solution [23]. When a droplet micelle solution of low concentration (1 mg/ml) was cast onto the coverglass, the solvents flowed radially toward the perimeter by capillary flow. Most of the micelle particles were then brought towards the peripheral region of the droplet by the radial flow and a ring was formed as shown in Fig. 2. With reference to Fig. 2, the ring is observed with fission gaps. This could be ascribed to the volume contraction upon drying. For increased concentrations of micelle solution (5 mg/ml), on the contrary, micelles will be distributed throughout the drying surface. Then, the primary cracks will be initiated from the drying edge and further penetrate towards the center of the drying droplet into unidirectional channel-like structure, as shown in Fig. 1(A).

When the concentration of the micelle solution increased from 5 to 10 mg/ml, secondary cracks were nucleated at the wall of the primary cracking. The secondary cracks, which penetrated into the middle of the strap pattern, propagated in

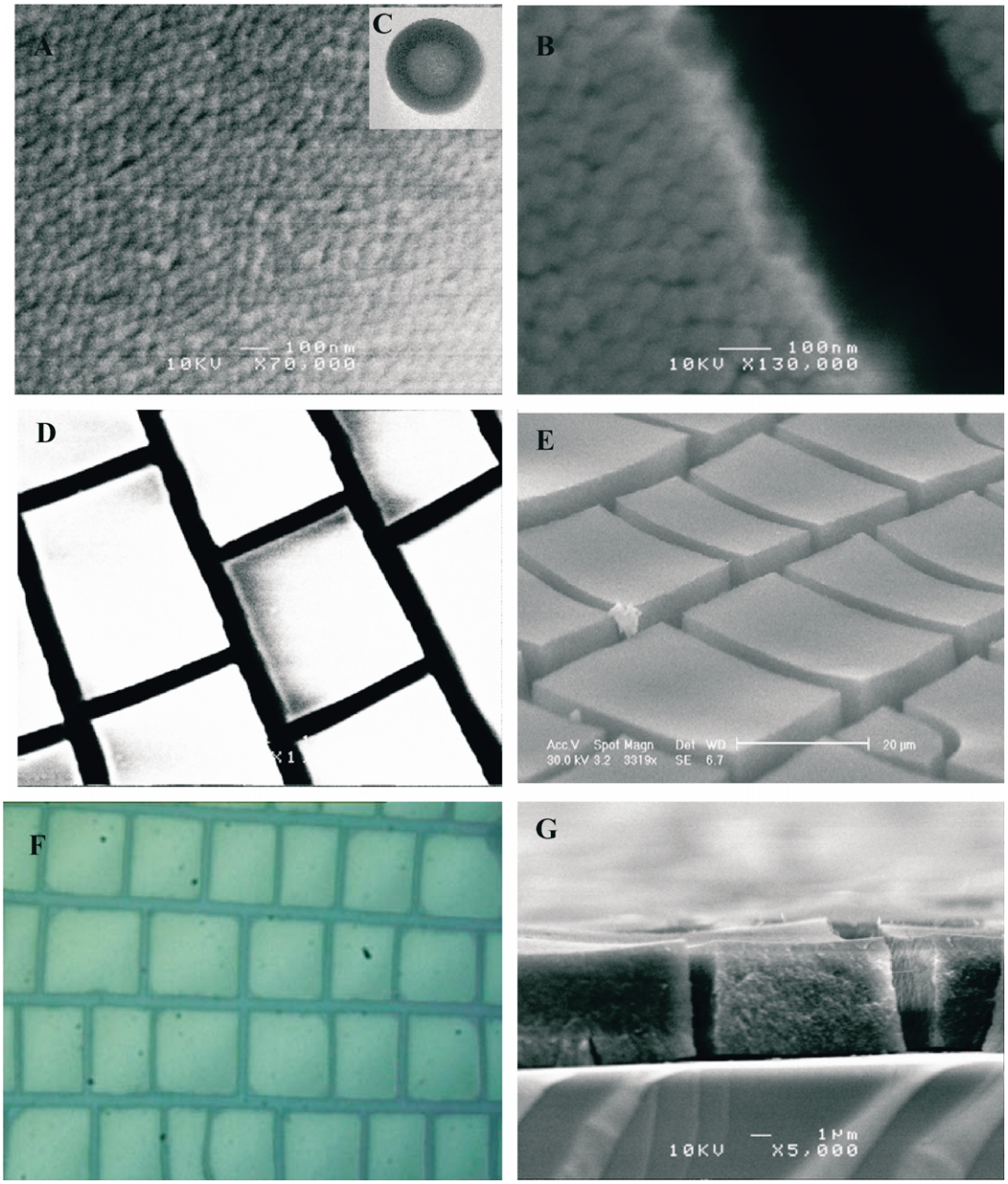

Fig. 3. The SEM micrographs of aggregated micelles (A) and (B). The TEM micrograph showing a single micelle with a diameter of 30 nm (C). The SEM micrographs of the diblock copolymer micropatterns induced by evaporation (D) and (E). The OM image of the micropatterns (F). The cross-section SEM micrograph of the crack blocks of the micropattern (G).

a direction perpendicular to the primary crack, parallel to the drying edge of the solution droplet. The secondary cracking stopped as they met the next primary crack. The combined primary and secondary cracks resulted in an orderly aligned tiling pattern of quadrate block. The process of primary and secondary crack development was recorded by the digital video camera (Sony 3CCD color video camera).

Fig. 3(A) and (B) shows the SEM micrographs of the closely packed micelles aggregation upon drying. Fig. 3(C) is the TEM micrograph of a single micelle with a diameter of 30 nm. The observation was found corresponding to the previous studies on the crack pattern formation of drying films [24–28]. However, our experiment has revealed some new phenomena. Crack patterns with higher degree of regularity were achieved. Micropatterns with square and rectangular structures were shown in Fig. 3(D)–(G). In addition to the quadrate structures, a number of interesting patterns have also been developed.

For the investigation of the crack pattern, we used an Alpha-Step 200 profiloer system to study the surface topology of the micropatterns. The system is able to

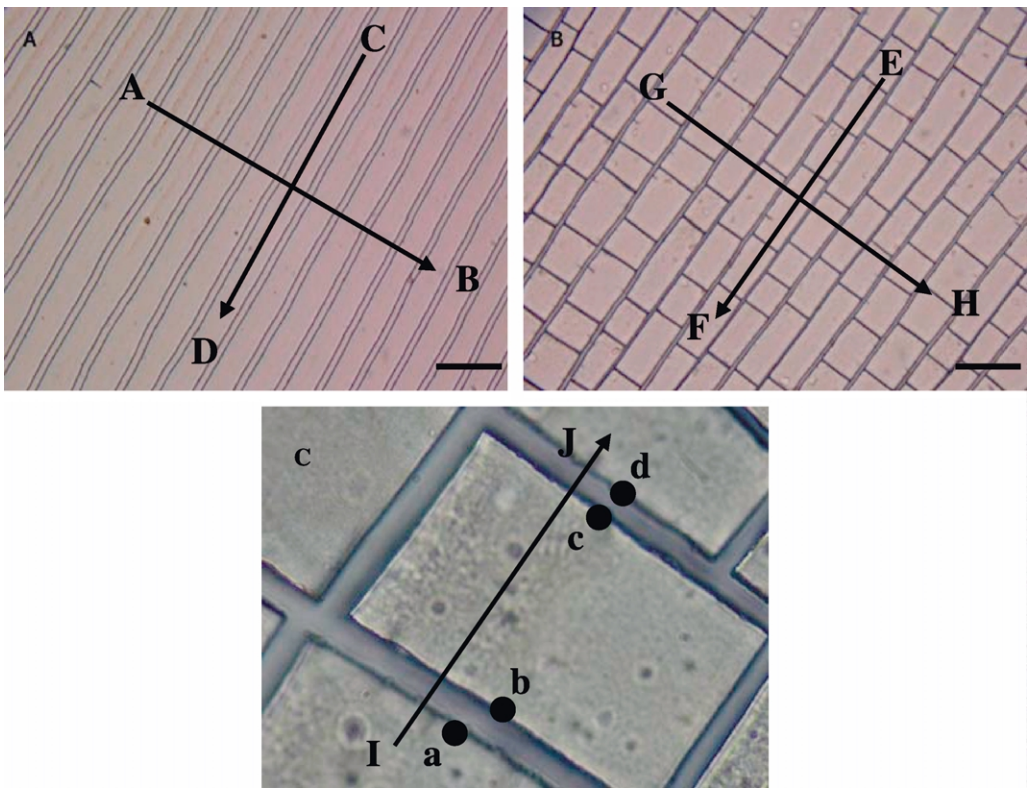

Fig. 4. The scanning direction for the Alpha-Step 200 profiler.

investigate the vertical range of the depth from 1000 Å to 1000 kÅ with a resolution of 50 Å. The scan length is 3 mm. This equipment measures surface profiles by scanning a mechanical stylus across the sample. The scanning directions are indicated, in Fig. 4(A)–(C), as *AB*, *CD*, *EF*, *GH*, and *IJ*, respectively. A series of results of the Alpha-Step 200 profiler system are shown in Fig. 5(A)–(D). The abscissa is the scan length in μm and the ordinate is the vertical depth in kÅ. It is observed from Fig. 5(A) that the surface topology across the strap patterns along AB in Fig. 4(A) is periodically undulating. The topological period shown in Fig. 5(A) corresponds to the width of the strap in Fig. 4(A) in the direction *AB*. When scanning in the direction of *CD* in Fig. 4(A), it is found that the surface is relatively flat and the scanned result is shown in Fig. 5(B). This flat surface supports the previous discussion that, when the micelle concentration is low, strap pattern will be formed and will leave a relatively flat surface in the radial direction.

When scanning in the direction of GH in Fig. 4(B), the result resembled the undulation as that shown in Fig. 5(A). When the scan was in the direction of EF, however, in contrast to the result attained in Fig. 5(B), we found the surface is undulating periodically as shown in Fig. 5(C). A better view of the surface topology of the farmland structure is shown in Fig. 5(D), which is resulted from scanning in the direction of IJ in Fig. 4(C). The dot positions of *a*, *b*, *c*, and *d* in Fig. 4(C) correspond to the positions of *a*, *b*, *c*, and *d* as indicated in Fig. 5(D). In Fig. 5(D), ab and cd represent the gap. The discontinuity of the curves in Fig. 5(A), (C) and (D) is due to the gaps that are too deep for the tip to reach the bottom. The surface topology of the farmland pattern is best represented by the curve bc in Fig. 5(D). With reference to Figs. 1(D), 5(C) and (D), one can easily notice that the farmland patterns share the following characters in common: each block with an area of about 1000 μm^2 and the surface topology of each pattern block is concave in the center. The concave depth measured at the center of the pattern is about 1000–2000 Å as shown in Fig. 5(C) and (D). These characters offer some ideas in the possible applications of the farmland structure.

In addition to the quadrate farmland structure of the diblock copolymer micropatterns, a number of biologically resembling structures were also achieved. Figs. 6(A)–(I) show the versatile micropatterns with biomimetic structures we have obtained with the PS–PAA diblock copolymer micelles. Also in Fig. 6, we make a comparison between the biomimetic structures of the diblock copolymer micelles and several biological images. The small inserts at the lower right corner of each picture, Figs. 6(a)–(i), are the raphides in the cortex cells in Fig. 6(a), the cross-section of plant root and its endodermis in Figs. 6(b) and (c), the tracheids in the parenchyma in Figs. 6(d) and (e), the collenchyma in Fig. 6(f), the chloroplasts in Fig. 6(g), and the cells in telophase and plasmolysis in Figs. 6(h) and (i). The result of Fig. 6

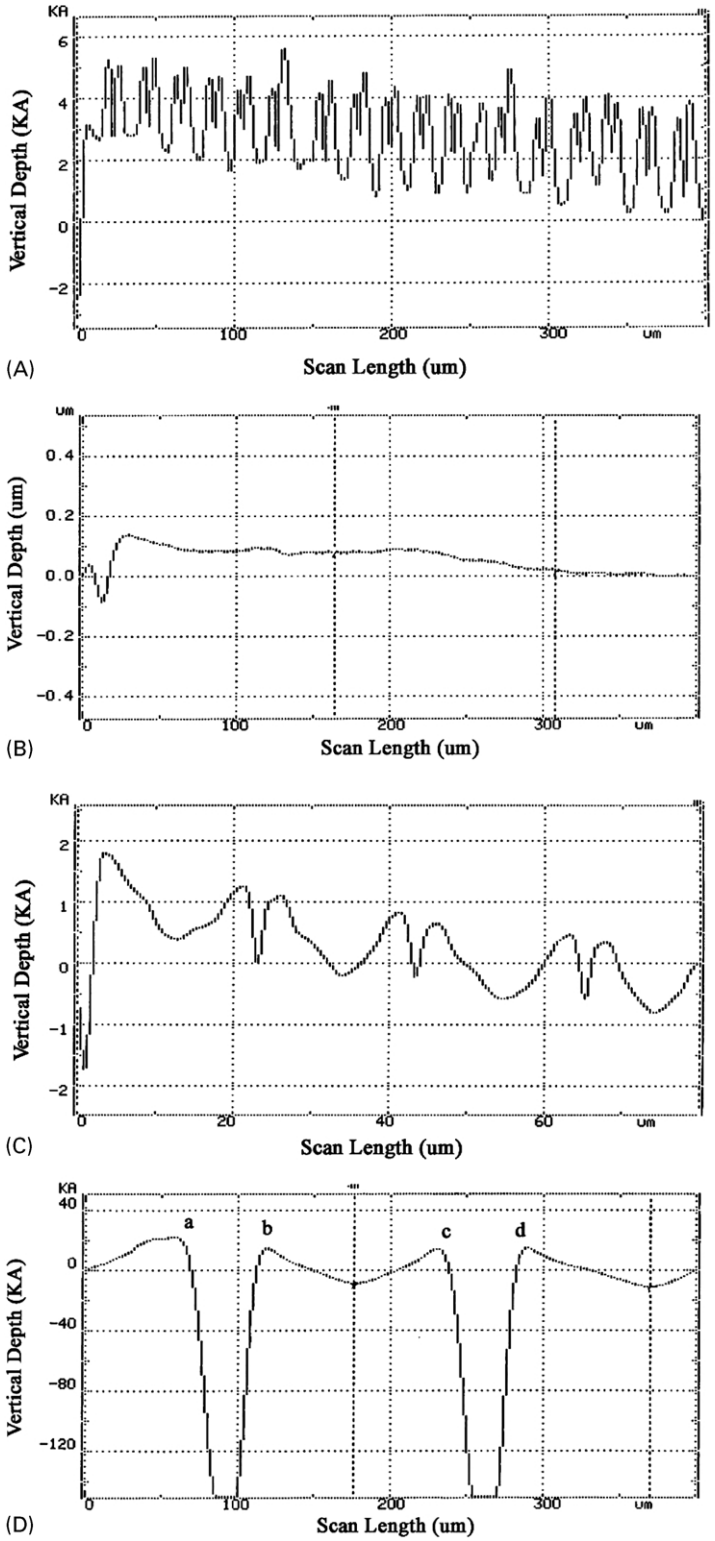

Fig. 5. (A) The surface topology as scanned by the Alpha-Step 200 profiler along the direction AB in Fig. 4(A). (B) The surface topology as scanned by the Alpha-Step 200 profiler along the direction CD in Fig. 4(A). (C) The surface topology as scanned by the Alpha-Step 200 profiler along the direction EF in Fig. 4(B). (D) The surface topology as scanned by the Alpha-Step 200 profiler along the direction IJ in Fig. 4(C). The samples studied by the Alpha-Step 200 profiler were the micropatterns of PS-b-PDMS diblock copolymer.

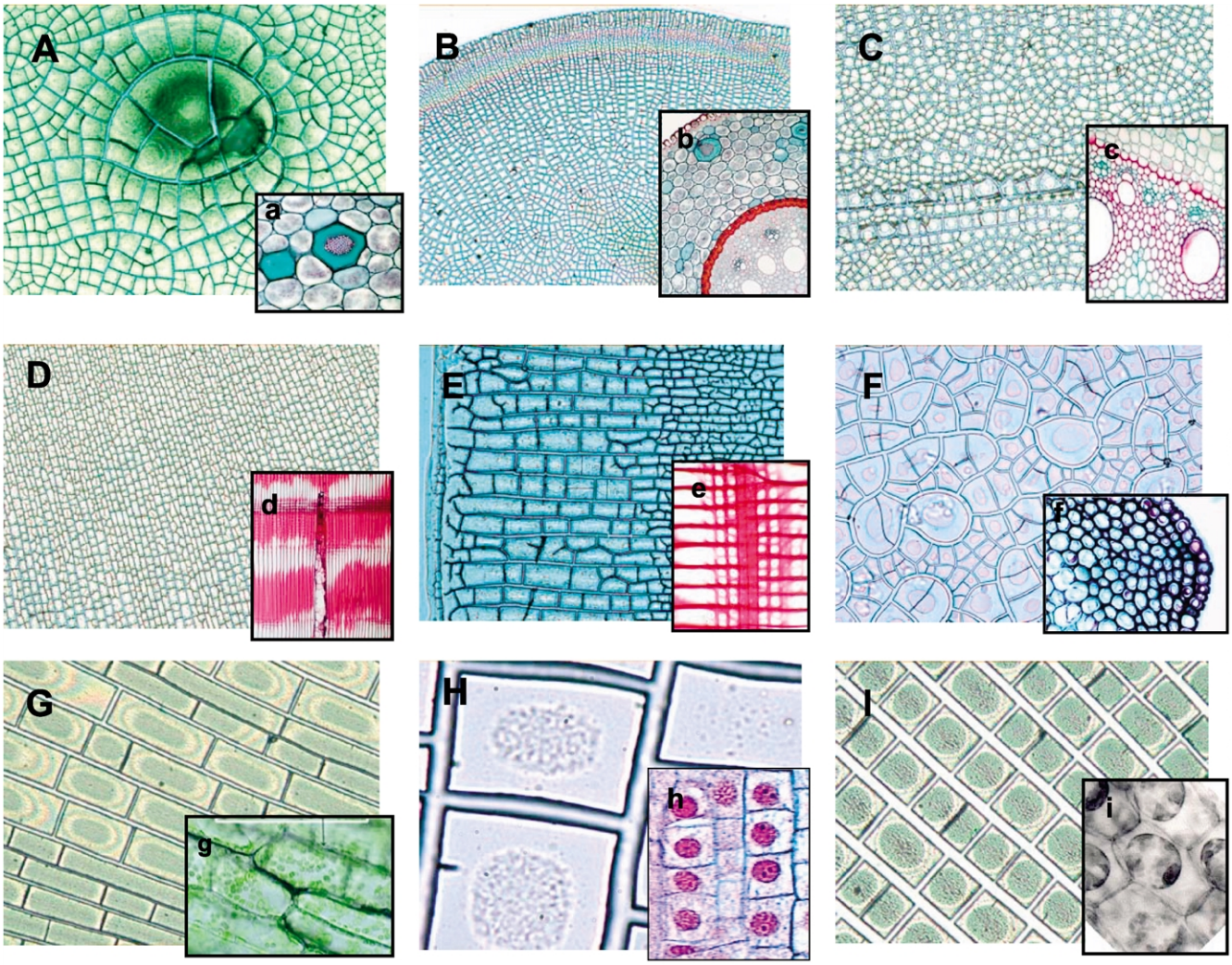

Fig. 6. The versatile diblock copolymer micropatterns with different biomimetic structures (A)–(I), and the corresponding micrographs of animals and plants tissue for comparison (a)–(i).

demonstrates a certain degree of analogy of the diblock copolymer micropatterns to the nature biological patterns.

4. Significance of this work

We believe that the regular micropatterns can be obtained in larger scale by controlling the evaporation speed and evaporation condition, micelle solution concentration, micelles morphology and the surface condition of the substrate. Micropatterns with controllable regularity are expected and will have potential applications in biosensors and bio-analytics, biomedical engineering, micro-electronics, and micro-bioreactors.

To date, most of the substrate platform for bioanalytical application is dominated by the moulding or microfabrication technology. The molded plastics surface for bioanalytics was claimed to be relatively less efficient because of the large size of the sample wells. For the advanced microfabrication technology, well-organized tiny wells of milli- or micron-scale are achieved by photo or chemical etching on silicon wafer surface under a contaminant-free environment. Usually, this industrial practice requires professional labor, huge investment on the sophisticated equipment, and spacious laboratory. In contrast, this research offers a rapid, inexpensive and efficient alternative. The micropattern thus obtained is a regularly ordered structural array whose scale is 100 times smaller than the micro titer plates which are widely employed by the nowadays clinical laboratory. Here, we report that the micropattern can be obtained by a one-step evaporation process within minutes. The fabrication of the analytical-chip can be simply performed by a simple micromolding technique using the micropattern as templates. In addition, we are currently directing our research to immobilize antibodies and DNA probes onto polystyrene microparticles and to embed the PS microparticles on the micromolded high-density micro-titer plate. We wish to design and establish a fast analytical method by a microparticle-in-well system

that behaves as a multi-analytical immunoassay microchip or DNA microarray for biochemistry tests.

Acknowledgements

Research grant RGC HKUST6195/01P is greatly acknowledged.

References

[1] Hamley TW. The physics of block copolymers. NY: Oxford University Press; 1998.
[2] Zhang L, Eisenberg A. Science 1995;268:1728.
[3] Zhang L, Eisenberg A. J Polym Sci, Part B: Polym Phys 1999;37:1469.
[4] van der Schoot P, Wittmer JP. Macromol Theory Simul 1999;8:428.
[5] Liu H, Anna J, Jian G, Kathryn EUR. J Polym Sci, Part A: Polym Chem 1999;37:703.
[6] Park M, Harrison C, Chaikin PM, Register RA, Adamson DH. Science 1997;276:1401.
[7] Heath JR. Science 1995;270:1315.
[8] Khandpur AK, Forster S, Bates FS. Macromolecules 1995;28:8796.
[9] Bashir R. Superlattices Microstruct 2001;29:1.
[10] Martin CR. Science 1994;266:1961.
[11] Chen ZR, Kornfield JA, Smith SD, Grothaus JT, Satkowski MM. Science 1997;277:1248.
[12] Templin M, Franck A, Du Chesne A, Leist H, Zhang Y, Ulrich R, Schadler V, Wiesner U. Science 1997;278:1795.
[13] Liu G, Ding J, Qiao L, Guo A, Dymov BP, Gleeson JT, Hashimoto T, Saijo K. Chem Eur J 1999;5:2740.
[14] Wooley KL. J Polym Sci, Part A: Polym Chem 2000;38:1397.
[15] Ding J, Liu G. J Phys Chem B 1998;102:6107.
[16] Jones MC, Leroux JC. Eur J Pharm Biopharm 1999;101.
[17] Kwon GS, Okano T. Adv Drug Deliv Rev 1996;21:107.
[18] Gref R, Minamitake Y, Peracchia MT, Trubetskoy V, Torchilin V, Langer R. Science 1994;263:1600.
[19] Kataoka K, Togawa H, Harda A, Yasugi K, Matsumoto T, Katayose S. Macromolecules 1996;29:8556.
[20] Rager T, Meyer WH, Wegner G. Macromol Chem Phys 1999;200:1672.
[21] Tian M, Qin A, Ramireddy C, Webber SE, Munk P. Langmuir 1993;9:1741.
[22] Forster S, Zisenis M, Wenz E, Antonietti M. J Chem Phys 1996;104:9957.
[23] Deegan RD, Bakajin O, Dupont TF, Huber G, Nagel SR, Witten TA. Nature 1997;389:827.
[24] Groisman A, Kaplan E. Europhys Lett 1994;25:415–20.
[25] Allain C, Limat L. Phys Rev Lett 1995;74:2981–4.
[26] Jagla EA. Phys Rev E 2002;65:046147.
[27] Pauchard L, Adda-Bedia M, Allain C, Couder Y. Phys Rev E 2003;67:027103.
[28] Shorlin KA, Bruyn JR, Graham M, Morris SW. Phys Rev E 2000;61(6):6950–7.